# Removal of microcystin-LR from aqueous solution using *Moringa oleifera* Lam. seeds

Rabia Yasmin, Kiran Aftab and Muhammad Kashif


## ABSTRACT

The removal of microcystin-LR from aqueous solution using native *Moringa oleifera* Lam. seeds powder (MSP) and chemically pretreated *M. oleifera* Lam. seed powder (PMSP) was investigated in terms of equilibrium and kinetics. Optimum sorption conditions were determined as a function of pH (2–7), adsorbent dosage (0.25–1.0 g/L), initial concentration of microcystin-LR (15–120 mg/L) and contact time (15–360 minutes). The high values of regression constant, 0.98 (MSP) and 0.99 (PMSP), revealed that sorption of microcystin-LR was best fitted by the pseudo second order kinetic model. The equilibrium study was best fitted by the Freundlich model with both the adsorbents. The maximum sorption capacity by MSP and PMSP for microcystin-LR was 85.5 ± 1.1 mg/g and 92.49 ± 2.4 mg/g respectively. Fourier transform infrared spectroscopy showed the major involvement of carboxyl and hydroxyl groups for microcystin-LR sequestration either by complexation or ion exchange mechanism. The contribution of the adsorption phenomenon was confirmed by scanning electron microscopic analysis of microcystin-LR loaded and unloaded PMSP. Thus, the HCl-pretreated *M. oleifera* Lam. seed powder proved to be the pre-eminent biosorbent for removal of microcystin-LR from the wastewater stream.


**Key words** | Freundlich model, kinetic study, microcystin-LR, *M. oleifera* seeds, pretreatment

**Rabia Yasmin**
**Kiran Aftab** (corresponding author)
Department of Chemistry,
Government College Women University
Faisalabad,
Faisalabad,
Pakistan
E-mail: *kiranaftab@gcwuf.edu.pk*

**Muhammad Kashif**
Department of Mathematics and Statistics,
University of Agriculture Faisalabad,
Faisalabad,
Pakistan

## NOMENCLATURE

| | |
|---|---|
| MSP | Native *M. oleifera* seed powder |
| PMSP | HCL treated *M. oleifera* seed powder |
| $R_L$ | Separation factor, dimensionless |
| b | Langmuir constant |
| $C_1$ | Final microcystin-LR concentration (mg/L) |
| $C_o$ | Initial microcystin-LR concentration (mg/L) |
| $C_e$ | Equilibrium microcystin-LR concentration (mg/L) |
| $K_2$ | Pseudo second order rate constant |
| $K_F$ | Freundlich adsorption capacity |
| n | Adsorption intensity |
| q | Sorption capacity (mg/g) |
| $q_e$ | Amount of sorption at equilibrium (mg/g) |
| $q_{max}$ | Maximum amount of microcystin-LR per unit mass (mg/g) |
| $q_t$ | Amount of sorption at time 't' (mg/g) |
| V | Volume of microcystin-LR solution (L) |
| W | Weight of adsorbent (g) |

## INTRODUCTION

Cyanobacterial blooms or cyanotoxins are widely classified as hepatotoxins (microcystins, cylindrospermopsin and nodularin), neurotoxins (anatoxins, saxitoxins and homoanatoxins-a) and dermatotoxins on the basis of structure and toxicity. Among them, microcystins are the most common and widely studied cyanobacterial toxin, and can be produced by *Microcystis*, *Planktothrix*, *Anabaena*, *Oscillatoria* and *Nostoc*. Microcystins are highly stable in aquatic environments under normal conditions, can tolerate high temperature and are found to be more toxic (Zheng *et al.* 2016).

Three primary environmental factors – temperature, light exposure and high concentrations of nitrogen and phosphorus – promote the formation of cyanobacterial blooms (Merel *et al.* 2013). Due to MC toxicity, the World Health Organization set a provisional drinking water guideline value of 1 μg microcystin-LR per litre (Li *et al.* 2016). For children the permissible guideline value is 0.4 μg

doi: 10.2166/wst.2019.006

microcystin-LR per litre (He *et al.* 2016). Microcystins are cyclic heptapeptides that can inhibit the protein phosphatase of type 1 and type 2A and thus are called hepatotoxins. Long-term ingestion of microcystin can cause liver damage, hepatotoxicity, cytotoxicity and neurotoxicity (Lian *et al.* 2014; Zamyadi *et al.* 2015).

Among 80 variant microcystins, microcystin-LR is found to be most abundant and toxic in nature. The structure of microcystin-LR reported by Jiang *et al.* (2014) includes two unusual amino acids (3-amino-9-methoxy-2,6,8-trimethyl-10-phenyldeca-4,6-dienoic acid and N-methyldehydroalanine, three D-amino acids (glutamic acid, alanine and methylaspartic acid) and two variable L-amino acids X and Z which are leucine and arginine.

Due to human health concern there is a strong need to remove microcystins from drinking water resources. For this purpose various physical and chemical methods are used to remove microcystins from aqueous solutions. Coagulation, flocculation and filtration are found to be more effective in the removal of cyanobacterial toxins. An increase in the dose of coagulant can effectively destroy the harmful disinfection byproduct precursors like natural organic matter (He *et al.* 2016). The traditional coagulation/flocculation process shows disturbance in cyanotoxins removal due to their low density, negative surface charge and morphological properties. Therefore, a pre-oxidation step is required to increase the effectiveness of these conventional methods. For this purpose many oxidants or algaecides, including chlorine, chlorine dioxide, chloramines and ozone, are used (Fan *et al.* 2013).

Pre-oxidation by using chlorine is not found to be very efficient because of release of toxins and cell lysis. Moreover, ozonation also has some disadvantages due to synthesis of toxic byproducts and is more time-consuming.

The most convenient method for the removal of microcystin-LR is to use natural products such as *Moringa oleifera* Lam *M. oleifera* Lam. seed extracts are highly effective in clarification of turbid water, act as a natural coagulant and can remove hydrophobic organic pollutants from water resources. Due to antimicrobial properties *M. oleifera* seed extracts can also stop the cell growth and were found to be very effective in the coagulation process (Gopalakrishnan *et al.* 2016).

The present study was conducted to investigate the removal of microcystin-LR, using native and HCl pretreated *M. oleifera* Lam. seed powder, from aqueous solution to develop a cost-effective greener technology. The effects of several physico-chemical parameters were also evaluated to optimize the sorption process. In addition, the experimental data were analyzed by isotherms and the kinetic models.

## MATERIALS AND METHODS

### Collection of samples

The adsorption properties of the powdered seed of an indigenous *M. oleifera* Lam. were investigated for removal of microcystin-LR from aqueous solution. For this purpose *M. oleifera* seeds were collected from Herbyzone Pakistan Limited, Lahore, Pakistan. All the other chemicals used were of analytical grade.

### Preparation of adsorbents

A domestic blender was used to grind *c.*20 g of seeds into a fine powder (MSP). One half of the was modified with a chemical approach. MSP (10 g) was treated with 25 mL HCl (0.1 M) at temperature 30 °C and 100 rpm on an orbital shaker (PAMICO Technologies) for 6 hours. Then the sample was filtered, washed thoroughly, and dried in a thermostatic drying oven (DHG-9030A Series Thermal-Electric) till constant weight. The pretreated *M. oleifera* seed powder (PMSP) was stored in air-tight Falcon conical tubes for further use.

### Adsorbents characterization

The proximate analysis of the adsorbents was carried out to determine volatile matter, ash contents and moisture contents. The pore volume, the pore size distribution and the specific surface area of the native MSP and HCl treated MSP samples were determined by nitrogen absorption using Brunauer–Emmett–Teller (BET) analysis. Nitrogen at 77 K is considered to be a standard adsorbent for surface area and pore size analysis. The BET specific surface area and the volume of monolayer coverage were determined using the BET equation.

The solid addition method was used to examine the zero surface charge properties of MSP and PMSP (Kumar *et al.* 2008). Fifty millilitres of potassium nitrate (0.1 M) solution was used in a series of 100 mL conical flasks. The $pH_0$ values of the solutions were adjusted and noted from 1 to 12 by addition of HCl (0.1 M) or NaOH (0.1 M). MSP (1 g) was added to each flask, which was then capped quickly. Then the suspensions were allowed to equilibrate

for 24 hours with manual shaking and the $pH_f$ values of the supernatant liquid from each flask were noted.

Fourier transform infrared (FTIR) spectroscopy and scanning electron microscopy were used to analyze the involvement of different functional groups and morphological characteristics of the adsorbent surface before and after biosorption (Dotto *et al.* 2013).

### Analytical measurements

High performance liquid chromatography with a UV detector at 238 nm was used to analyze the concentration of microcystin-LR, following the reported method of Lian *et al.* (2014). The removal efficiency of microcystin-LR before and after incubation was observed by comparison of peak area ratios of microcystin-LR.

### Batch experimental study

Batch sorption experiments were performed in a set of Erlenmeyer flasks (250 mL) where solutions of microcystin-LR (100 mL) with different initial concentrations (15–120 mg/L) were interacted with adsorbents (MSP and PMSP) having 0.25–1.00 g/L pulp density, maintaining the initial pH in the range of 2 to 7. The pH of the solutions was adjusted to the required value by adding either 0.1 M HCl or 0.1 M NaOH solution. These mixtures were agitated at 100 rpm shaking speed (temperature controlled shaker, PAMICO Technologies) at 30 °C for 2 hours. A time course study was carried out by pipetting out a 5.0 mL sample from experimental flasks at specified time intervals of 0.25, 0.5, 1.0, 2.0 and 6.0 hours. The concentration of microcystin-LR in the supernatant solution before and after adsorption was determined using high performance liquid chromatography with a UV detector at 238 nm, and C18 analytical column having size 4.5 mm × 200 mm for the remaining microcystin-LR concentration. The sample was centrifuged for 5 minutes for analysis. The supernatant was used for residual microcystin concentration.

The percentage removal efficiency of microcystin-LR was expressed as:

$$\%\ \text{removal of microcystin-LR} = C_o - C_1/C_o \times 100$$

where $C_o$ is the initial microcystin-LR concentration (mg/L) and $C_1$ is the equilibrium concentration of microcystin-LR in bulk solution (mg/L). The equilibrium adsorption capacity, $q_e$ (mg/g), was calculated by the following formula:

$$(q_e) = (C_o - C_1)V/W$$

where V is the volume of the solution (mL) and W is the mass of the adsorbent in grams.

All experiments were performed in duplicate.

### Statistical analysis

Comparative importance of all the factors (initial pH of solution, initial concentration of microcystin-LR, time and adsorbent dosage) were evaluated through factorial design. The factorial design would expose the effect of the interaction of process variables and improve the optimization process. The interactions between independent factors were determined with analysis of variance (ANOVA) and the main effects of microcystin-LR adsorption were identified based on the *P*-value with >95% confidence level. The results of the experimental design were analyzed using MINITAB 17 statistical software to evaluate the effects as well as the statistical parameters and the statistical plots.

### Adsorption isotherms and kinetic study

The data obtained from removal of microcystin-LR on *M. oleifera* seeds powder were examined by simulating the adsorption isotherms through the Langmuir and Freundlich equations.

The experimental data pertaining to time course studies were subjected to pseudo first order, second order and pseudo second order kinetic models. The model-predicted values were validated by correlation coefficient $R^2$ values along with comparison of the theoretical value with the experimental one.

## RESULTS AND DISCUSSION

### Adsorbent characterization

The physical and chemical properties of MSP and PMSP were estimated through proximate analysis including the determination of moisture contents (%), volatile matter (%), ash contents (%) and fixed carbon (%) contents as shown in Table 1. The respective values for MSP and PMSP were 6.69% and 8.98% moisture content, 5.86%

and 4.30% volatile matter, 8.73% and 3.69% ash content, and 78.72% and 83.03% fixed carbon.

The BET surface areas and Barrett–Joyner–Halenda (BJH) pore size distribution of both native and HCl pretreated adsorbents were analyzed. The results of the BJH analysis showed the behavior of adsorptive $N_2$ within the pores is subject to pore network and blockage effects. For native MSP, BJH pore area was found to be 57.304 $m^2/g$ for pore size range 17–3,000 Å. The BJH average pore diameter was 165.633 Å while the BET average pore width was 574.995 Å. HCl pretreated MSP pore size analysis displayed dominance over the external surface. For PMSP a pore area (BJH) of 193.146 $m^2/g$ with pore size range 17–3,000 Å was observed. The average pore width (BET) was 9590.222 Å while the average pore diameter (BJH) was 183.167 Å. The predominance of the microporous structure was clarified by the analysis of both native and pretreated MSP. PMSP was found to have significant impact on the isotherm behavior at low relative pressure.

Point of zero charge (PZC) is of fundamental importance in surface science to determine the acidity/basicity and net surface charge of adsorbent in solution. The difference between the $pH_0$ and $pH_f$ values ($\Delta pH$) was plotted against the $pH_0$. The point of zero charge was obtained at the point of intersection of the resulting curve, at which $\Delta pH = 0$. The $pH_{PZC}$ for native MSP was found to be as 4.0 and for PMSP was found to be 2.9 as shown in Figure 1.

**Table 1** | Characteristics of native and pretreated *M. oleifera* seed powder

| Adsorbent characteristics | MSP | PMSP |
|---|---|---|
| Proximate analysis | | |
| Moisture contents (%) | 6.69 | 8.98 |
| Volatile matter (%) | 5.86 | 4.30 |
| Ash contents (%) | 8.73 | 3.69 |
| Fixed carbon (%) | 78.72 | 83.03 |
| Surface area ($m^2/g$) analysis | | |
| BET | 16.49 | 3.68 |
| Single point | 14.99 | 3.43 |
| BJH cumulative adsorption | 57.30 | 193.1 |
| Pore volume ($cm^3/g$) | | |
| BJH cumulative adsorption | 0.23 | 0.88 |
| Single point | 0.23 | 0.88 |
| Pore size (Å) | | |
| Average pore width (BET) | 574.9 | 9,590.2 |
| Average pore diameter (BJH) | 165.6 | 183.1 |

This difference in $\Delta pH_{PZC}$ shows the variations in the surface functional groups of the native MSP and PMSP.

## Factors affecting adsorption study

The pH affects the adsorption capacity due to its influence on the surface properties of adsorbent and ionic form of microcystin-LR. Therefore, sorption capacity of native and pretreated *M. oleifera* Lam. seed powder (0.5 g/L) was investigated to study the effect of initial solution pH (2–7) with 100 mL of 15 mg/L microcystin-LR solution for 30 minutes at 100 rpm and 30 °C temperature. Maximum percentage removal of microcystin-LR onto MSP (68.4%) and PMSP (80.9%) was found to occur at pH 3 as shown in Figure 2.

The high efficiency of MSP and PMSP at lower pH may be justified according to Huang *et al.* (2007) as hydrogen bonding among the coiled molecules of microcystin-LR lowers the toxin's water solubility and subsequently increases its affinity for sorbent surface. PMSP surface due

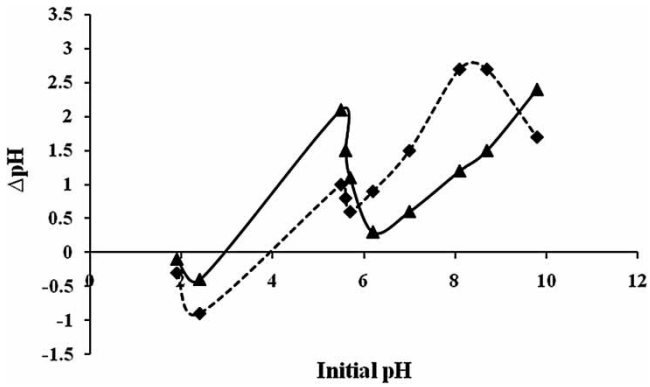


**Figure 1** | Determination of the point of zero charge ($pH_{PZC}$) of MSP (◆) and PMSP (▲) through solid addition method.

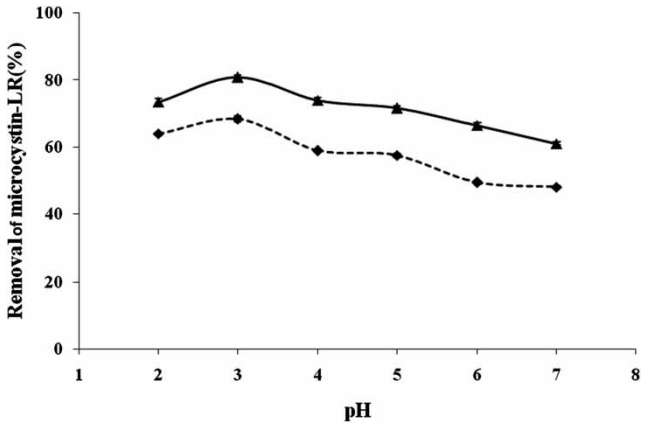


**Figure 2** | Effect of pH on removal efficiency of microcystin-LR through adsorbents MSP (◆) and PMSP (▲).

to pretreatment would be carrying cationic charges that cause ion pairing effect more electrostatic attraction and showed 12% higher adsorption than MSP. The PMSP surface showed 12% higher adsorption than MSP due to the pretreatment, which results in the PMSP carrying cationic charges that cause ion pairing effect and more electrostatic attraction. A similar trend of high sorption capacity at low pH was also reported for adsorption of microcystin-LR using synthetic magnetic bentonite material (Lian *et al.* 2014) and peat (Sathishkumar *et al.* 2010). Microcystin-LR removal with MSP and PMSP was 48.08% and 61.12% respectively at pH 7 and these values are almost 20% less at pH 3.0.

ANOVA analysis results are shown in Table 2 where *P*-value <0.05 shows significant effects for factor 1 and factor 2 while no interaction exists between these factors as *P*-value is greater than 0.05. Tukey test for comparison of means was performed with 95% confidence level (Table 3).

**Table 2** | Percentage removal of microcystin-LR with native and pretreated *M. oleifera* Lam. seed powder at various pH

| Variable | Removal of microcystin-LR (%) |
|---|---|
| Factor 1 | |
| HCl pretreated *M. oleifera* seed powder | 71.32[a] |
| Native *M. oleifera* seed powder | 55.23[b] |
| Factor 2 | |
| pH 3 | 74.66[a] |
| pH 2 | 68.79[a,b] |
| pH 4 | 66.51[a,b] |
| pH 5 | 64.63[a,b] |
| pH 6 | 68.04[b,c] |
| pH 7 | 47.02[c] |

Small letters represent comparison between interaction means. The means followed by different superscripted lowercase letters (a–c) indicate significant differences ($P < 0.05$) based on ANOVA two-way factorial test.

**Table 3** | Percentage removal of microcystin-LR at different adsorbent dosage with native and pretreated *M. oleifera* Lam. seed powder

| | Microcystin-LR removal (%) | |
|---|---|---|
| Adsorbent dose (g/L) | MSP | PMSP |
| 0.25 | 46.49[f] | 61.55[e] |
| 0.5 | 68.41[c] | 80.93[a] |
| 0.75 | 65.65[d] | 73.59[b] |
| 1.00 | 66.90[c,d] | 72.52[b] |

Small letters represent comparison between interaction means. The means followed by different superscripted lowercase letters (a–f) indicate significant differences ($P < 0.05$) within the rows and columns based on two-way factorial ANOVA followed by Tukey's test.

Significant effects were shown at pH 3 and pH 7 with highest mean value at pH 3 and lowest at pH 7. High percentage removal of negatively charged microcystin-LR anions from aqueous solution was observed at low values of pH, because the adsorbent surface carries greater number of positive charged adsorption sites at lower pH. At pH 7, the presence of hydroxyl ions decreases the adsorption of microcystin-LR due to competition between microcystin-LR anions and hydroxyl ions. Similar results were obtained in dye removal by Safa & Bhatti (2011) using agriculture waste.

## Effect of adsorbent dosage

The effect of biosorbent dosage on the percentage removal of microcystion-LR was studied. A hundred millilitres of 15 mg/L microcystin-LR solution was used, which was incubated for 30 minutes, adding variable amounts of adsorbent (0.25, 0.5, 0.75 and 1 g/L) (Figure 3).

The values of percentage removal first increased sharply by increasing adsorbent concentration from 0.25 to 0.5 g/L for both the adsorbents giving 68.4% and 80.9% removal for MSP and PMSP respectively at pulp density value of 0.5 g/L. With the increase in adsorbent concentration from 0.5 to 1.0 g/L, no further increase in percentage removal was observed. Change in adsorbent dosage shows significant effects on the adsorption process as confirmed through ANOVA and Tukey test for comparison shown in Table 3. Similarly, a small decrease in values of sorption capacity was also observed with increase in adsorbent dose from 0.5 g/L to 1.0 g/L; maximum value of sorption capacity was found to be $20.52 \pm 0.8$ and $22.71 \pm 1.3$ mg/g for MSP and PMSP respectively at 0.5 g/L adsorbent concentration.

This descending trend would be a result of smaller amount of sorbent surface available for microcystin-LR

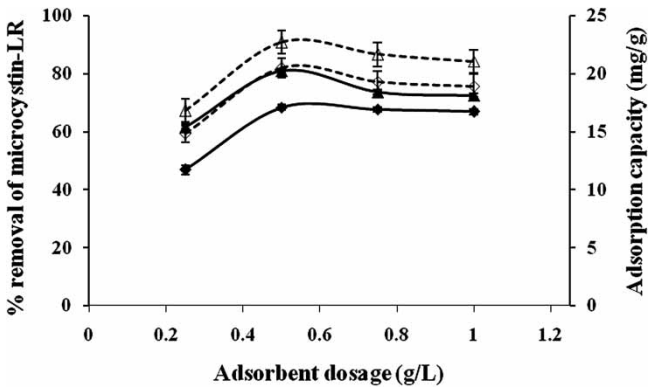


**Figure 3** | Microcystin-LR uptake capacity and % removal by MSP (◇, ◆) and PMSP (△, ▲) as a function of adsorbent concentration ($C_o = 15$ mg/L, volume = 100 mL, contact time = 30 minutes at room temperature).

**Table 4** | Maximum sorption capacities for microcystin-LR uptake by different sorbents

| Biosorbents | $q_{max}$ (mg/g) | References |
|---|---|---|
| Carbon nanotubes | 05.9 | Yan *et al.* (2004) |
| Coconut shell activated carbon | 16.6 | Huang *et al.* (2007) |
| Wood-based activated carbon | 83.3 | Huang *et al.* (2007) |
| Magnetophoretic nanoparticle of polypyrrole | 91.51 | Hena *et al.* (2016) |
| Nanozero-valent iron @chitosan | 68.9 | Yang *et al.* (2018) |
| Polysulfone biomass composite fiber | 40.24 | Kim *et al.* (2018) |
| *Moringa* seed powder | 85.5 | Present study |
| Pretreated *Moringa* seed powder | 92.49 | Present study |

**Table 5** | Pseudo second order kinetic model, rate constant and $q_e$ for microcystin-LR adsorption at initial concentration 15 mg/L, pH = 3 and 0.05 g/100 mL

| Pseudo second order parameters | MSP | PMSP |
|---|---|---|
| $q_e$ (mg/g) | 98.7 | 101.8 |
| $K_2$ | 11.23 | 10.18 |
| $R^2$ | 0.98 | 0.99 |
| $q_{expt}$ (mg/g) | 85.5 | 92.49 |

$q_{expt}$: Experimental adsorption capacity; $q_e$: Theoretical adsorption capacity at equilibrium; $K_2$: Rate constant for pseudo second order kinetic model.

binding at high biomass concentration due to cell aggregation (Safa & Bhatti 2011). The results demonstrated that the amount of adsorbent strongly affected the removal of microcystin-LR from aqueous solution (Lian *et al.* 2014).

## Effect of contact time and initial concentration of microcystin-LR

Aqueous solutions of microcystin-LR having different initial concentration (15, 30, 60, 90 and 120 mg/L) were studied for contact time of 0.25, 0.5, 1.0, 2.0 and 6.0 hours to observe the sorption capacity ($q_e$) of MSP and PMSP. In Table 4 some already studied sorbents are summarized to make comparison of their maximum sorption capacities. The maximum uptake capacity of MSP and PMSP was $19.07 \pm 0.6$ and $20.78 \pm 0.5$ mg/g respectively at 15 mg/L initial concentration, which increased to $85.5 \pm 1.1$ and $92.49 \pm 2.1$ mg/g respectively at initial concentration of 120 mg/L at equilibrium. The sorption capacity increased prominently from $19.07 \pm 0.6$ to $55.3 \pm 0.7$ mg/g for MSP and from $20.78 \pm 0.5$ to $58.01 \pm 0.7$ mg/g for PMSP after 6 hours of contact time when initial microcystin-LR concentration was increased from 15 to 90 mg/L (Figure 4).

By increasing the initial concentration from 90 to 120 mg/L, slight increase in microcystin uptake after 6 hours of contact time was observed indicating that the binding sites were almost saturated. Increase in uptake capacity causes decrease in microcystin-LR removal percentage from 70.12% to 40.48% by MSP and from 76.42% to 43.76% by PMSP. Certainly it is not unreasonable to expect that at low concentration, the ratio of available surface to the initial microcystin-LR concentration is larger, so the removal becomes independent of initial concentrations. However, at higher concentrations the available surface area becomes less compared to the moles of adsorbate present. Hence the percentage removal was dependent upon the initial adsorbate concentration (Hena *et al.* 2014). Sathishkumar *et al.* (2010) also reported similar results for the removal of microcystin-LR by peat.

From the plot of the sorption capacity versus time it was observed that the microcystin-LR uptake capacity was only 70.12% with MSP, and in the case of PMSP the initial uptake rate was rapid reaching about 76.42% in the first 2 hours of contact time. It was only due to the accessibility of adsorbent surface area. Initially, a large accessible surface area is available to microcystin-LR; as a result the adsorption rate is high. The bare surface lessened rapidly with increasing coverage, and competition for sorption sites take place. Thus, with the passage of time the slower adsorption rate was observed, which leads to equilibrium.

Since the sorption of microcystin-LR remains almost constant, a steady-state approximation was implicated after 120 minutes. The smaller size of particles and larger pore size of PMSP make it more available to microcystin-LR by diffusion from solution, compared with MSP. Significant change in residual microcystin-LR concentration is observed at 120 minutes: 70.12% removal by MSP and 76.42% removal by PMSP.

## Kinetic modeling of microcystin-LR

Adsorption kinetics of microcystin-LR on MSP and PMSP was studied using 15 mg/L initial concentration of microcystin-LR at initial pH 3 of aqueous solution. The observed data for the adsorption of microcystin-LR fit very well to the pseudo second order kinetic model with high correlation coefficient values (0.98 and 0.99) for MSP and PMSP (Table 5).

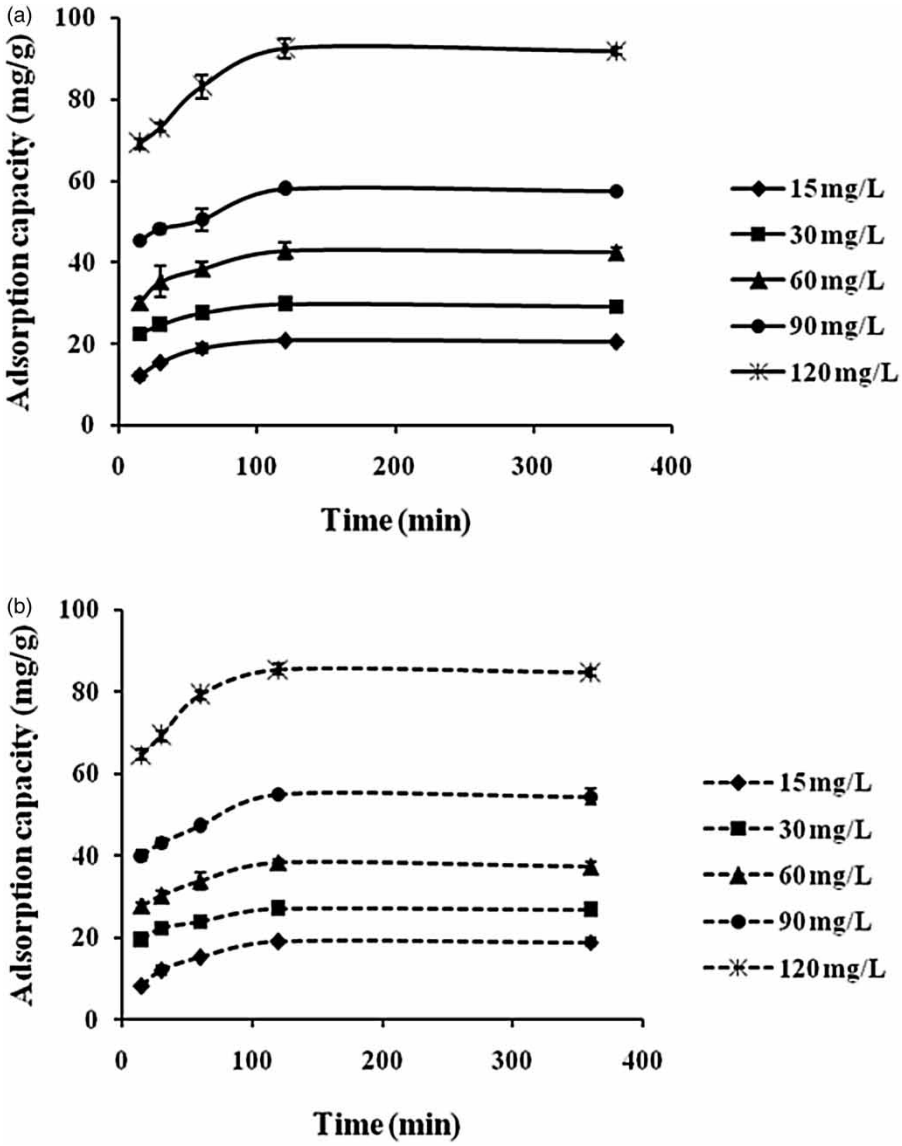


**Figure 4** | Time course studies on the effect of various initial concentrations of microcystin-LR on sorption on MSP (a) and PMSP (b) (0.05 g in 100 mL volume at room temperature).

The pseudo second order kinetic model can be described by the following equations:

$$t/q_t = 1/K_2 q_e^2 + t/q_e$$

As q represents the amount of microcystin-LR adsorbed on adsorbent (mg/g), $q_e$ and $q_t$ represent the amount of microcystin-LR adsorbed at equilibrium and time *t* respectively. $K_2$ is the rate constant for the pseudo second order kinetic model.

The values of $K_2$ (g/mg.min) and $q_e$ (mg/g) were calculated from the slope and intercept of straight lines, obtained by plotting $t/q_t$ against t for microcystin-LR adsorption (Figure 5). The values of correlation coefficients from the pseudo second order plot were high and theoretical values of $q_e$ were in good agreement with experimental $q_e$. However, for PMSP the value of $q_e$ obtained from the pseudo second order kinetic model showed greater harmony with the experimental $q_e$ value as compared those values for MSP for microcystin-LR sorption.

## Isothermal studies

The Langmuir and Freundlich equations were used to simulate the equilibrium adsorption isotherms to obtain the

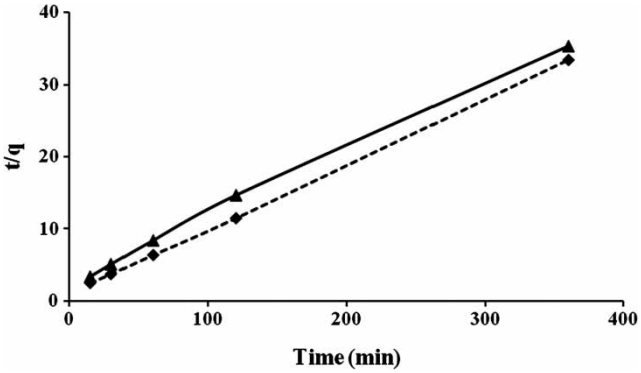


**Figure 5** | Pseudo second order kinetic plot of microcystin-LR sorption using MSP (♦) and PMSP (▲) at room temperature.

adsorption capacity of *M. oleifera* seeds for microcystin-LR. The Langmuir isotherm is expressed as:

$$1/q_e = 1/q_{max} + 1/bq_{max}C_e$$

where $q_e$ (mg/g) is the equilibrium adsorption capacity, $C_e$ (mg/L) is the equilibrium concentration of microcystin-LR in the solution, $q_{max}$ (mg/g) is the adsorption capacity, and b (L/mg) is the Langmuir constant. The essential characteristics of the Langmuir isotherm can be described by a dimensionless constant called the separation parameter, $R_L$, which is defined by the following equation:

$$R_L = 1/(1 + bC_0)$$

Favorable adsorption is reported when the $R_L$ values are between 0 and 1 (El Mouzdahir *et al.* 2007). The Freundlich adsorption isotherm can be expressed as:

$$\ln q_e = \ln K_f + 1/n \ln C_e$$

where $K_F$ and n are Freundlich adsorption isotherm constants related to the adsorption capacity and the adsorption intensity respectively.

The values of correlation coefficients from Langmuir plots were 0.95 for MSP and 0.98 for PMSP (Figure 5) at various initial concentrations of microcystin-LR. The values of $q_{max}$ and b were calculated from the intercept and slope of the straight lines and are given in Table 6. The values of $q_{max}$ were not in agreement with experimental values in the case of MSP and PMSP. Langmuir plots for microcystin-LR sorption using MSP and PMSP adsorbents showed that the model was not noticeably followed by any adsorbent. The essential feature of the Langmuir isotherm is separation factor ($R_L$). The $R_L$ value for microcystin-LR sorption with both adsorbents ranges from 0 to 1.0 as shown in Table 6.

**Table 6** | Isothermal study for microcystin-LR adsorption onto native and pretreated *M. oleifera* Lam. seed powder

| Adsorption isotherm parameters | MSP | PMSP |
|---|---|---|
| $q_{expt}$ (mg/g) | 85.5 | 92.49 |
| Langmuir | | |
| $q_{max}$ (mg/g) | 4.27 | 35.71 |
| $R^2$ | 0.95 | 0.98 |
| b | 40 | 0.04 |
| $R_L$ | 0.12 | 0.62 |
| Freundlich | | |
| $q_{max}$ (mg/g) | 104.5 | 94.93 |
| $R^2$ | 0.83 | 0.99 |
| $K_F$ | 8.55 | 17.5 |
| n | 1.71 | 2.35 |

$q_{expt}$: Adsorption capacity at equilibrium; $q_{max}$: Maximum adsorption capacity; b: Langmuir constant; $K_F$ and n: Freundlich constant.

Similarly the values of correlation coefficients from Freundlich plots were 0.83 for MSP and 0.99 for PMSP at various initial concentrations of microcystin-LR. The values of $K_F$ and n were calculated from the intercept and slope of the straight lines and are given in Table 6. The values of Freundlich $q_{max}$ were in harmony with experimental values in the case of MSP, while for PMSP the experimental $q_{max}$ value is almost the same as the Freundlich $q_{max}$ value, unlike that of the Langmuir isotherm.

The greater deviation observed in the Langmuir model may be because the microcystin-LR sorption was due to non-interactive binding of microcystin-LR to the adsorbent surface in the Langmuir model, compared to multilayer sorption in the Freundlich isotherm. The irregular pattern of isotherm and sorption may be due to the complex nature and presence of multiple active sites on the adsorbent. An $R_L$ value greater than 0 and less than 1 indicates a favorable sorption process (Aftab *et al.* 2015).

## FTIR analysis

The nature of PMSP and microcystin-LR interactions was elucidated by recording the FTIR spectra (Thermo Nicolet, Model Magna 760) in the range of 450–4,000 $cm^{-1}$ of unloaded and loaded adsorbents following 2 hours of contact time.

In the FTIR spectra of adsorbents before and after microcystin sorption, the appearance of multiple absorption bands at 3,050–3,500 $cm^{-1}$ showed the involvement of –OH and –NH groups of the adsorbents. The broad band

positioned around 3,280 $cm^{-1}$ and 3,289 $cm^{-1}$ was assigned to the stretching vibration of -NH amide groups. These peaks attest to the high content of protein present in *Moringa* seeds. The strong absorbance at 2,922 $cm^{-1}$ and 2,923 $cm^{-1}$ in both spectra are assigned to symmetrical and asymmetrical stretching of the C-H ($CH_2$). A peak at 2,067 $cm^{-1}$ shows alpha-beta unsaturated alkyl groups in unloaded PMSP; this peak is absent in the spectra of microcystin-LR loaded PMSP indicating the involvement of this group in microcystin sorption. In the region between 1,800 and 1,600 $cm^{-1}$ there are three intense bands assigned to C=O bond stretching. The carbonyl group is present in the fatty acid and protein structures. In the case of unloaded PMSP and microcystin-LR loaded PMSP, the spectra show two bands at 1,745 $cm^{-1}$ and 1,710 $cm^{-1}$ associated with fatty acids, and a band at 1,654 $cm^{-1}$ and 1,646 $cm^{-1}$ confirmed the major contribution of the amide group in the sorption process. The presence of a peak at 1,541 $cm^{-1}$ in both spectra can be assigned to N-H deformation which confirms the presence of the amide group. The presence of this band confirms the protein structure in the *Moringa* seeds (Araujo *et al.* 2010).

The bands at 1,236 and 1,058 $cm^{-1}$ in PMSP spectra are associated with the carboxylic vibrations and stretching of phenols in PMSP spectra; however, these bands are absent in microcystin-LR loaded PMSP spectra, which provide adsorption sites. According to Meneghel *et al.* (2014) plant residues are basically composed of macromolecules (e.g., lignin, cellulose, hemicellulose and protein) which have adsorptive sites able to adsorb microcystin-LR. A peak at 718 $cm^{-1}$ appeared in microcystin-LR loaded PMSP spectra, showing aromatic C-H deformation, while no peak was observed in this range in PMSP spectra. This peak may be attributable to the fact that the aromatic character increases in microcystin-LR loaded spectra compared with PMSP.

### SEM analysis

For the further investigation of adsorption phenomena, the unloaded and microcystin-LR loaded PMSP were investigated under a scanning electron microscope (SEM). Scanning electron microscopy is a useful technique that produces digital magnified images (micrographs) of an object, and can be used to show the natural adsorbent morphology and its alteration after adsorbate interactions (Nurchi *et al.* 2010). SEM micrographs of unloaded (Figure 6(a)) and loaded (Figure 6(b)) adsorbents showed a significant surface difference. SEM analysis of microcystin-LR loaded biomass showed the presence of dense particles.

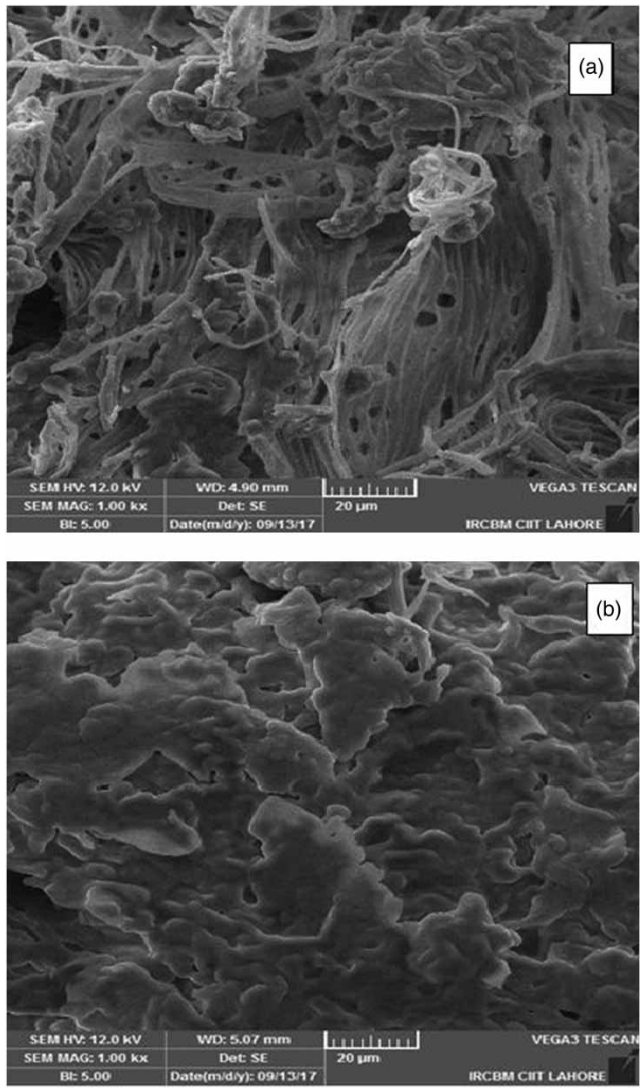


**Figure 6** | Scanning electron micrographs of unloaded pretreated *Moringa* seed powder (a) and 15 mg/L microcystin-LR solution loaded pretreated *Moringa* seed powder (b).

## CONCLUSIONS

The present work makes the comparision between native and HCl treated *M. oleifera* seeds for removal of microcystin-LR from aqueous solutions. It could be concluded that PMSP was found to be more effective than MSP for the removal of microcystin-LR from aqueous solution under optimized pH 3, adsorbent dosage 0.5 g/L and initial microcystin-LR concentration 15 mg/L. The maximum sorption capacity for PMSP was 92.4 ± 2.4 mg/g. The sorption process is multilayered as the observed experimental data were best fitted to the Freundlich isotherm model. The pseudo second order model endorsed all experimental

results as its $R^2$ value is near 1. Characterization of seeds and the sorption process showed that the PMSP has great potential for microcystein-LR removal from water. Moreover, the process is simple, so economically accessible and attractive. However, further research in technical aspects of the process is a requisite for commercial application of this batch study.

## REFERENCES


Aftab, K., Akhtar, K. & Anjum, F. 2015 Removal and recovery of lead ($Pb^{2+}$) from industrial effluent using indigenous and tailor-made *Aureobasidium* sp. RBSS-303. *Water Science and Technology* **71** (1), 139–148.

Araujo, C. S., Alves, V. N., Rezende, H. C., Almeida, I. L., de Assuncao, R. M., Tarley, C. R. T., Segatelli, M. G. & Coelho, N. M. M. 2010 Characterization and use of *M. oleifera* seeds as biosorbent for removing metal ions from aqueous effluents. *Water Science and Technology* **62** (9), 2198–2203.

Dotto, G. L., Costa, J. A. V. & Pinto, L. A. A. 2013 Kinetic studies on the biosorption of phenol by nanoparticles from *Spirulina* sp. LEB 18. *Journal of Environmental Chemical Engineering* **1** (4), 1137–1143.

El Mouzdahir, Y., Elmchaouri, A., Mahboub, R., Gil, A. & Korili, S. 2007 Adsorption of methylene blue from aqueous solutions on a Moroccan clay. *Journal of Chemical and Engineering Data* **52** (5), 1621–1625.

Fan, J., Ho, L., Hobson, P. & Brookes, J. 2013 Evaluating the effectiveness of copper sulphate, chlorine, potassium permanganate, hydrogen peroxide and ozone on cyanobacterial cell integrity. *Water Research* **47** (14), 5153–5164.

Gopalakrishnan, L., Doriya, K. & Kumar, D. S. 2016 *M. oleifera*: a review on nutritive importance and its medicinal application. *Food Science and Human Wellness* **5** (2), 49–56.

He, X., Liu, Y.-L., Conklin, A., Westrick, J., Weavers, L. K., Dionysiou, D. D. & Walker, H. W. 2016 Toxic cyanobacteria and drinking water: impacts, detection, and treatment. *Harmful Algae* **54**, 174–193.

Hena, S., Ismail, N., Isaam, A. M., Ahmad, A. & Bhawani, S. A. 2014 Removal of microcystin-LR from aqueous solutions using % burn-off activated carbon of waste wood material. *Journal of Water Supply: Research and Technology-AQUA* **63** (5), 332–341.

Hena, S., Rozi, R., Tabassum, S. & Huda, A. 2016 Simultaneous removal of potent cyanotoxins from water using magnetophoretic nanoparticle of polypyrrole: adsorption kinetic and isotherm study. *Environmental Science and Pollution Research* **23** (15), 6540–6545.

Huang, W.-J., Cheng, B.-L. & Cheng, Y.-L. 2007 Adsorption of microcystin-LR by three types of activated carbon. *Journal of Hazardous Materials* **141** (1), 115–122.

Jiang, W., Chen, L., Batchu, S. R., Gardinali, P. R., Jasa, L., Marsalek, B. & Sharma, V. K. 2014 Oxidation of microcystin-LR by ferrate (VI): kinetics, degradation pathways, and toxicity assessments. *Environmental Science & Technology* **48** (20), 12164–12172.

Kim, S., Yun, Y. S. & Choi, Y. E. 2018 Development of waste biomass based sorbent for removal of cyanotoxin microcystin-LR from aqueous phases. *Bioresource Technology* **247**, 690–696.

Kumar, A., Paradas, B. & Mishra, I. M. 2008 Adsorptive removal of acetonitrile by commercial grade activated carbon: kinetics, equilibrium and thermodynamics. *Journal of Hazardous Materials* **152**, 589–600.

Li, X., Cheng, R., Shi, H., Tang, B., Xiao, H. & Zhao, G. 2016 A simple highly sensitive and selective aptamer-based colorimetric sensor for environmental toxins microcystin-LR in water samples. *Journal of Hazardous Materials* **304**, 474–480.

Lian, L., Cao, X., Wu, Y., Sun, D. & Lou, D. 2014 A green synthesis of magnetic bentonite material and its application for removal of microcystin-LR in water. *Applied Surface Science* **289**, 245–251.

Meneghel, A. P., Goncalves Jr, A. C., Tarley, C. R. T., Stangarlin, J. R., Rubio, F. & Nacke, H. 2014 Studies of $Pb^{2+}$ adsorption by *M. oleifera* Lam. seeds from an aqueous medium in a batch system. *Water Science and Technology* **69** (1), 163–169.

Merel, S., Walker, D., Chicana, R., Snyder, S., Baures, E. & Thomas, O. 2013 State of knowledge and concerns on cyanobacterial blooms and cyanotoxins. *Environment International* **59**, 303–327.

Nurchi, V. M., Crisponi, G. & Villaescusa, I. 2010 Chemical equilibrium in wastewaters during toxic metal ion removal by agricultural biomass. *Coordination Chemistry Reviews* **254**, 2181–2192.

Safa, Y. & Bhatti, H. N. 2011 Adsorptive removal of direct textile dyes by low cost agricultural waste: application of factorial design analysis. *Chemical Engineering Journal* **167** (1), 35–41.

Sathishkumar, M., Pavagadhi, S., Vijayaraghavan, K., Balasubramanian, R. & Ong, S. 2010 Experimental studies on removal of microcystin-LR by peat. *Journal of Hazardous Materials* **184** (1), 417–424.

Yan, H., Gang, P., Hua, Z., Xianliang, L. & Hao, C. 2004 Effective removal of microcystins using carbon nanotubes embedded with bacteria. *Chinese Science Bulletin* **49** (16), 1694–1698.

Yang, X., Wei, X., Xu, X. & Liu, Z. 2018 E3S Web of Conferences 53, 04004, *ICAEER 2018*. https://doi.org/10.1051/e3sconf/20185304004.

Zamyadi, A., Coral, L. A., Barbeau, B., Dorner, S., Lapolli, F. R. & Prevost, M. 2015 Fate of toxic cyanobacterial genera from natural bloom events during ozonation. *Water Research* **73**, 204–215.

Zheng, B., Fu, H., Berry, J. P. & McCord, B. 2016 A rapid method for separation and identification of microcystins using capillary electrophoresis and time-of-flight mass spectrometry. *Journal of Chromatography A* **1431**, 205–214.


First received 7 September 2018; accepted in revised form 13 December 2018. Available online 8 January 2019